Heartbeat Classification Using Morphological and Dynamic Features of ECG Signals

Can Ye*, *Student Member, IEEE*, B. V. K. Vijaya Kumar, *Fellow, IEEE*, and Miguel Tavares Coimbra, *Member, IEEE*

***Abstract*—In this paper, we propose a new approach for heartbeat classification based on a combination of morphological and dynamic features. Wavelet transform and independent component analysis (ICA) are applied separately to each heartbeat to extract morphological features. In addition, RR interval information is computed to provide dynamic features. These two different types of features are concatenated and a support vector machine classifier is utilized for the classification of heartbeats into one of 16 classes. The procedure is independently applied to the data from two ECG leads and the two decisions are fused for the final classification decision. The proposed method is validated on the baseline MIT-BIH arrhythmia database and it yields an overall accuracy (i.e., the percentage of heartbeats correctly classified) of 99.3% (99.7% with 2.4% rejection) in the "class-oriented" evaluation and an accuracy of 86.4% in the "subject-oriented" evaluation, comparable to the state-of-the-art results for automatic heartbeat classification.**

***Index Terms*—Heartbeat classification, independent component analysis, support vector machine, wavelet transform.**

I. Introduction

COMPUTER-ASSISTED electrocardiogram (ECG or EKG) interpretation has been an intense research focus for decades. Research advances in automatic ECG analysis have made positive contributions to the timely detection and better management of cardiac disorders in clinical situations.

Cardiac arrhythmias refer to a large group of conditions in which there is abnormal activity or behavior in heart [1]. Some types of arrhythmia are life-threatening medical emergencies that can trigger cardiac arrest and sudden death, such as ventricular fibrillation and tachycardia. Detection of such arrhythmias has been well investigated [2]–[4].

Manuscript received November 24, 2011; revised February 29, 2012, April 23, 2012 and July 6, 2012; accepted July 10, 2012. Date of publication August 15, 2012; date of current version September 14, 2012. This work was supported by the Fundação para a Ciência e a Tecnologia (Portuguese Foundation for Science and Technology) under Student Grant SFRH/BD/33519/2008 and under Vital Responder Project Grant CMU-PT/CPS/0046/2008. *Asterisk indicates corresponding author*.

*C. Ye is with the Department of Electrical and Computer Engineering, Carnegie Mellon University, PA 15213 USA and also with the Instituto de Telecomunicações, Department of Computer Science, Faculty of Science, University of Porto, Porto 4099, Portugal (e-mail: cany@ece.cmu.edu).

B. V. K. Vijaya Kumar is with the Department of Electrical and Computer Engineering, Carnegie Mellon University, PA 15213 USA (e-mail: kumar@ece.cmu.edu).

M. T. Coimbra is with the Instituto de Telecomunicações, Department of Computer Science, Faculty of Science, University of Porto, Oporto 4099, Portugal (e-mail: mcoimbra@dcc.fc.up.pt).

Color versions of one or more of the figures in this paper are available online at http://ieeexplore.ieee.org.

Digital Object Identifier 10.1109/TBME.2012.2213253

In this study, we have investigated the detection of another group of arrhythmias, which might not be critically life-threatening but still need attention and therapy to avoid deterioration. An essential step toward detecting and classifying arrhythmias is the classification of heartbeats, given that heart rhythm category can be determined by the recognition of classes of consecutive heartbeats [5]. Beat-by-beat human-based examination can be very time-consuming and tedious to be practical in many scenarios. Besides, automatic ECG analysis is significant in long-term online monitoring of cardiac activity for timely detection of abnormal heart conditions, in which case the human monitoring and interpretation is unable to satisfy real-time diagnosis requirements. Therefore, automatic heartbeat classification of ECG signals can be instrumental in the diagnosis of cardiac arrhythmias and is the focus of investigation in this paper.

In the recent past, there have been numerous works [6]–[17] reported on automatic heartbeat classification. These works explored the characterization of heartbeats using a variety of features, including Hermite coefficients [6], [9], [13], high-order statistics features [9], [17], wavelet features [11], [14], waveform shape features [8], [10], [12], [15]– [17], etc. A number of machine learning algorithms have been proposed for classification, such as self-organizing map (SOM) [6], linear discriminats (LDs) [8], [12], [15], decision tree [10], support vector machine (SVM) [9], [11], artificial neural network (ANN) [13], [14], dynamic Bayesian network (DBN) [16], conditional random field (CRF) [17], etc. The algorithms were validated through the baseline MIT-BIH arrhythmia database [18].

The relevant literature [6]–[17] can be categorized into two different types based on the adopted evaluation scheme, namely, "class-oriented" and "subject-oriented." The "class-oriented" evaluation was adopted in most works, such as [6], [7], [9]–[11], [16]. The heartbeat segments were extracted from all or a few selected records of the MIT-BIH arrhythmias database and were clustered, based on the categorization of heartbeats. A certain fraction of each cluster (i.e., class) was selected as the training dataset and the remaining heartbeats were used as the testing dataset. Although it has been widely used for evaluation in the literature, it is worth noting that the "class-oriented" evaluation scheme is not a realistic measure of performance of automatic heartbeat classifier in real applications, leading to optimistic results since interindividual variation in ECG characteristics is less in such tests due to the fact that the training and testing datasets contain heartbeats from the same subjects, i.e., a similar beat might be included in the training dataset. However, in real applications, an ECG heartbeat classifier that performs well for a given training database could fail in predicting ECG signals

TABLE I
COMPARISON OF THE RESULTS FROM THE PROPOSED METHOD WITH PUBLISHED RESULTS [6]–[11]

Reference	Classes	Data Size	Features	Classifier	Fusion	Evaluation Scheme	Automatic Classifier
Lagerholm [6]	16	109,963	Hermite	Self-Organizing Map	No	class-oriented	Yes
Prasad [7]	13	105,423	Wavelet + RR	Neural Network	No	class-oriented	Yes
De Chazal [8]	5(16)	109,492	Waveform + RR	Linear Discriminants	Yes	subject-oriented	Yes
Osowski [9]	13	12,785	HOS + Hermite	Support Vector Machine	No	class-oriented	Yes
Rodriguez [10]	14	85,263	Waveform	Decision Tree	No	class-oriented	Yes
Jiang [11]	14	103,898	Wavelet + ICA	Support Vector Machine	No	class-oriented	Yes
De Chazal [12]	5(16)	109,492	Waveform + RR	Linear Discriminants	Yes	subject-oriented	No
Jiang [13]	5(16)	109,492	Hermite + RR	Block-based NN	No	subject-oriented	No
Ince [14]	5(16)	109,492	Wavelet + RR	Evolutionary ANN	No	subject-oriented	No
Llamedo [15]	5(16)	109,492	Waveform + RR	Linear Discriminants	Yes	subject-oriented	Yes
Oliveira [16]	2	14,080	Waveform + RR	Dynamic Bayesian Network	No	class-oriented	Yes
Lannoy [17]	5(16)	109,492	Waveform + HOS + RR	Conditional Random Field	No	subject-oriented	Yes
Proposed Method	**5(16)**	**110,109**	**Wavelet + ICA + RR**	**Support Vector Machine**	**Yes**	**class-oriented, subject-oriented**	**Yes**

from an "unobserved" individual, due to wild variations in ECG characteristics among different subjects and subject groups. A more realistic evaluation scheme, namely, the "subject-oriented" evaluation scheme, was proposed by De Chazal *et al.* [8] and adopted by recent works [15], [17]. The full database was divided into the training and the testing set based on records; the records in the training set were excluded from the testing set so that interindividual variation in ECG characteristics were taken into account, providing a more realistic estimate regarding the performance of heartbeat classifiers. The works [12]–[14] also adopted the "subject-oriented" evaluation. However, these works propose to build patient-specific heartbeat classifier. The beginning part (e.g., the first 5 min) of the particular individual record, termed as the individual training period, along with the manual beat annotations, is used for adapting the pretrained global classifier into a customized classifier. Although it usually yields significantly better performance with such adaptation, we have to note that manual labels of the individual training period require the external intervention, i.e., beat-by-beat annotation from cardiologists. Such external intervention makes the heartbeat classifier not fully automatic. Besides, the beat-by-beat annotation is expensive and time-consuming, making it impractical in most real applications. In this paper, both "class-oriented" and "subject-oriented" evaluation schemes are investigated. The design of "patient-specific" heartbeat classifier is not the focus and will not be discussed in this work. In summary, the "class-oriented" method is evaluated as a comparison with the literature results; the "subject-oriented" evaluation scheme is investigated as an estimate of potential performance of the proposed algorithm in clinical practice.

A comparative summary of these algorithms [6]–[17] as well as our proposed method can be seen in Table I. The primary differences derive from the following three aspects: feature extraction, classification, and two-lead fusion. For instance, in terms of feature extraction, wavelet, and ICA features have been utilized in [11]. In contrast with [11], where only approximation coefficients at level 4 are extracted as the wavelet features, we propose to utilize a combination of approximation coefficients at level 4 and detail coefficients at levels 3 and 4 as the wavelet features of heartbeats, since it corresponds to the frequency range of ECG signals, i.e., 0.5–40 Hz, as will be discussed in Section III. Jiang *et al.* [11] trained ICA components using 10 000 normal heartbeats, while in this study we have used hundreds of heartbeats from all of 16 classes, in order to improve our ability to describe the morphology of arrhythmias using these coefficients.

RR features has been widely employed in the literature, providing the characterization of temporal information of heartbeats. For most of the previous works [7], [13], [14], [16], two instantaneous RR features, also regarded as heartbeat interval features, were utilized namely, previous RR and post-RR features. De Chazal *et al.* [8] proposed another two RR features, i.e., local RR and average RR features, in addition to the two instantaneous RR features; this configuration was followed in [12], [17]. Although this idea is an interesting compact way to describe dynamic differences between beats, we will explain in Section III-F that some of these features, especially average RR, are not only unrealistic for online monitoring but also biased providing optimistic results.

In this work, the SVM is employed as the machine classification method. The probability estimates of each prediction are utilized to fuse the classification results from the two lead signals to make the final decision for each heartbeat, which turns out to be effective in making significant improvement over single-lead performance. In the literature, this was only done in [8], [12], [15], where the probability estimates from the two linear discriminant classifiers were utilized to fuse the prediction results from the two leads.

Motivated by this critical review of the previously most successful algorithms for heartbeat classification, this work proposes a new representation of heartbeats using a combination of improved morphological and dynamic features extracted from ECG signals. The motivation comes from a rule of thumb in clinical practice that ectopic heartbeats (arrhythmia heartbeats) can be distinguished from normal heartbeats in terms of both "morphology" and "dynamics" differences, as depicted in Fig. 1. Ectopic heartbeats can usually be characterized by various different abnormal or distorted patterns in the waveform shape (e.g., distorted QRS complex) or missing some important components (e.g., P wave) in one heart cycle. Besides, cardiac arrhythmias can typically be associated with and identified by various irregularities in heart rhythm. Based on this observation, we hereby propose to utilize the combination of morphological and dynamic features as the representation of the heartbeat, providing the characterization of the morphology of and the dynamics around the given heartbeat. It is worth noting that the morphological features used in this work are rather different

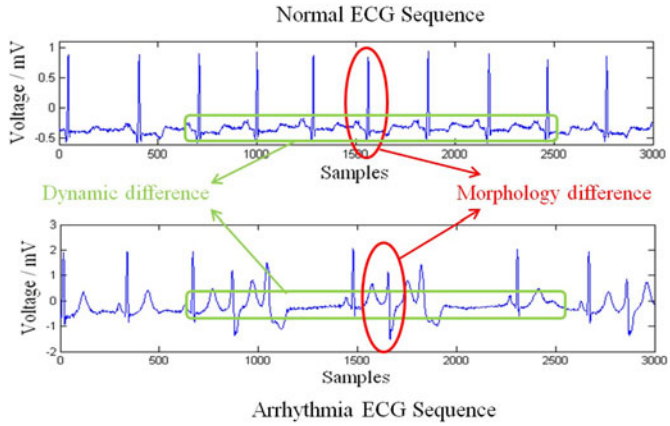

Fig. 1. Example for the illustration of the morphological and the dynamic differences between a normal beat and an ectopic beat.

from the waveform shape related features utilized in [8], [10], [12], and [15]–[17], which are defined as the duration or the interval between fiducial points, e.g., QRS duration, PR interval, etc. Instead, the morphological features investigated are obtained by expanding the heartbeat segment into two feature spaces, characterized by wavelets and ICA components as basis functions. Compared with the waveform shape-related features, the proposed morphological features provide a more complete representation regarding the morphology of the given heartbeat; moreover, the computation of waveform shape-related features requires the additional detection of other fiducial points besides R peak location, such as the onset and offset of T wave and P wave, which are usually sensitive to noise, possibly rendering this type of feature vulnerable in some ambulatory scenarios. Specifically, the resulting morphological features consist of the wavelet features (approximation coefficients at level 4 and detail coefficients at levels 3 and 4) and the ICA features, i.e., the weights on the trained ICA components. In addition to the morphological features, four improved RR interval related features are derived for each heartbeat to represent the dynamic characteristics in various scales. Consequently, each heartbeat is represented by the combined morphological and dynamic features. As we will see in Section IV, this proposed novel feature representation provides superior classification performance in distinguishing heartbeats from a variety of classes.

This paper extends our previous study [20] in the following aspects: 1) a more reasonable and realistic definition of local and average RR interval feature is utilized; 2) a new probabilistic estimate-based two-lead fusion approach is proposed to incorporate the two independent answers from the two single-lead SVM classifiers so as to determine the final classification answer; 3) both leave-one-out "record-by-record" cross validation and "subject-oriented" approaches are employed to evaluate the proposed method, providing a more realistic estimate of the performance in practice.

The rest of the paper is organized as follows: in Section II, the ECG dataset and the evaluation schemes are discussed; Section III presents theoretical background of the methodologies used and details of the experimental procedure; the experimental results, discussion as well as comparison with the published results are shown in Section IV; and conclusions are provided in Section V.

II. Dataset

A. Materials

The MIT-BIH arrhythmia database [18] was developed as the standard test material for the evaluation of arrhythmia detectors. The database is regarded as the benchmark database in arrhythmia detection and classification and has been extensively utilized for algorithm validation [6]–[17]. In this study, the performance of the proposed approach is also reported on this baseline database, allowing a direct comparison with published results.

The database contains 48 half-hour two-lead ambulatory ECG signals (denoted as lead A and lead B) from 47 subjects. Signals were band-pass filtered at 0.1–100 Hz and digitized at 360 Hz. Twenty-three records were chosen to contain normal sinus rhythm (NSR) and a representative set of routine arrhythmias; the other 25 records were selected to include less common but clinically significant cardiac abnormalities. In 45 recordings, the lead A signal is a modified limb lead II (MLII); the lead B signal is usually a modified lead V1 (occasionally V2 or V5, and in one instance V4). In the other three recordings, the lead A is V5 and the lead B is V2 (two instances) or MLII (one instance, i.e., signals were reversed). More detailed information regarding routine ECG lead placements can be found in [21].

We observe that the waveform shape varies among different lead configurations, i.e., sensor locations. For instance, heartbeats tend to have more prominent peaks in lead A signal than lead B signal. In addition, it is also noticed that ectopic beats seem to be more discernible than normal beats in lead B signal (e.g., in record 106). These observations motivate us to utilize both lead signals to make the decision, so as to improve the classification confidence.

There is an annotation file associated with each record, providing the reference annotations for each heartbeat, such as the location of the QRS complex and the category of the heartbeat. The category annotations are utilized as the ground truth for algorithm evaluation. The manual annotations of QRS locations are utilized for the segmentation of ECG signals, following the practice in the literature, so as to obtain heartbeat segments. Besides, an additional experiment is conducted by introducing certain artificial jitter to the annotated QRS locations, as an estimate of the potential error introduced by using a QRS detector, instead of using manual QRS annotations. The details of heartbeat segmentation will be discussed in Section III.

B. Evaluation Strategy

Two types of evaluation approaches are investigated in this paper, namely, "class-oriented" and "subject-oriented."

The "class-oriented" evaluation is conducted, to allow for the direct comparison with most published works, such as [6], [7], [9]–[11], [16]. In the "class-oriented" evaluation, all 48 records are used and heartbeat segments are obtained by segmenting

TABLE II
SUMMARY OF THE INFORMATION OF THE TRAINING AND TEST DATASETS IN CLASS-BY-CLASS EVALUATION SCHEME

Heartbeat Type	Annotation	Total #	Training Ratio	Training #	Test #
Normal Beat (NOR)	N	75017	13%	9753	65264
Left Bundle Branch Block (LBBB)	L	8072	40%	3229	4843
Right Bundle Branch Block (RBBB)	R	7255	40%	2902	4353
Atrial Premature Contraction (APC)	A	2546	40%	1019	1527
Premature Ventricular Contraction (PVC)	V	7129	40%	2852	4277
Paced Beat (PACE)	P	7024	40%	2810	4214
Aberrated Atrial Premature Beat (AP)	a	150	50%	75	75
Ventricular Flutter Wave (VF)	!	472	50%	236	236
Fusion of Ventricular and Normal Beat (VFN)	F	802	50%	401	401
Blocked Atrial Premature Beat (BAP)	x	193	50%	97	96
Nodal (Junctional) Escape Beat (NE)	j	229	50%	115	114
Fusion of Paced and Normal Beat (FPN)	f	982	50%	491	491
Ventricular Escape Beat (VE)	E	106	50%	53	53
Nodal (Junctional) Premature Beat (NP)	J	83	50%	42	41
Atrial Escape Beat (AE)	e	16	50%	8	8
Unclassifiable Beat (UN)	Q	33	50%	17	16
Total	16	110109	21.89%	24100	86009

ECG signals using the annotations of QRS location. The resulting heartbeat dataset are clustered into 16 clusters, each corresponding to one heartbeat class. The entire dataset was then split into training and testing datasets by randomly selecting a certain fraction from each of the 16 classes. Specifically, 13% of the beats from the normal class, 40% of the beats from each of five bigger arrhythmia classes (i.e., "L," "R," "A," "V," "P"), and 50% of the beats from each of ten smaller arrhythmias classes were randomly selected to constitute the training dataset, for a total of 21.89% beats of the whole dataset. The remaining heartbeats are utilized as the test dataset. The details of the 16 heartbeat classes as well as the datasets are summarized in Table II.

As discussed in Section I, the "class-oriented" evaluation leads to optimistic results. Therefore, the "subject-oriented" evaluation is conducted in addition as a more realistic estimate of generalization ability of the algorithm in practice. According to ANSI/AAMI EC57:1998 standard [19], the four paced records (i.e., the records 102, 104, 107, and 217) are excluded for experiments. The remaining 44 records are divided into the training and testing dataset, each consisting of 22 records, following the database division used in [8], [12], [15], and [17]. For the "subject-oriented" evaluation, the performance was reported in the five-class scheme recommended by ANSI/AAMI EC57:1998 standard [19], allowing direct comparison with published results. The original 16 heartbeat classes are reclustered into the five bigger classes, namely "N" (i.e., any heartbeat not in S, V, F, or Q classes), "S" (i.e., supraventricular ectopic beat), "V" (i.e., ventricular ectopic beat), "F" (i.e., fusion beat), and "Q" (i.e., unknown beat). The mapping from the MIT-BIH arrhythmia database heartbeat classes to the AAMI heartbeat classes is shown in Table III. In addition, the record-by-record cross validation is also conducted; basically, the dataset composed of 44 records is divided into 44 folds, with each fold consisting of heartbeat segments from one record. For each fold, the classifier is trained on the remaining 43 folds, and is utilized to predict the heartbeat data from the given fold. The process is iterated through all 44 folds.

TABLE III
MAPPING FROM MIT-BIH ARRHYTHMIAS HEARTBEAT CLASSES TO AAMI HEARTBEAT CLASSES

AAMI Classes	MIT-BIH Classes	Total #
N	NOR, LBBB, RBBB, AE, NE	90083
S	APC, AP, BAP, NP	2972
V	PVC, VE, VF	7480
F	VFN	802
Q	FPN, UN	15

III. METHODOLOGIES

Following the brief introduction of the proposed automatic heartbeat classification approach in Section I, we provide in this section a detailed description of the process and the theoretical background of the utilized techniques. Fig. 2 depicts the full process of the proposed method, which basically consists of five steps, namely, preprocessing, heartbeat segmentation, feature extraction, classification as well as two-lead fusion.

The raw ECG signals are first preprocessed to remove artifacts. Following the preprocessing, the ECG signals are subsequently divided into heartbeat segments, using provided R peak locations. Wavelet transform (WT) and independent component analysis (ICA) are separately applied to each heartbeat; and corresponding coefficients are concatenated and represented in a lower dimensional space using principal component analysis (PCA). The resulting principal components that account for most of the variance are selected, which are utilized to obtain a morphological descriptor of the heartbeat. In addition, a set of RR interval features are derived to obtain a characterization of the dynamics information around the particular heartbeat. Following the feature extraction, an SVM classifier is used for classifying heartbeats into 16 different classes. Given that the data from [18] contains two-lead ECG signals (denoted as lead A and lead B), the aforementioned procedure is independently applied to the signals from lead A and lead B. The two independent decisions derived for each heartbeat, are fused (using associated probabilities) to make the final decision of heartbeat classification. The classification confidence is improved by incorporating the signals from both leads for the final decision.

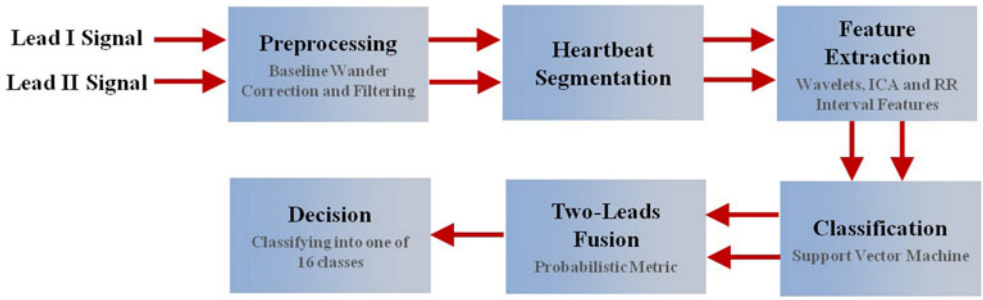

Fig. 2. Overview of the proposed automatic heartbeat classification methodology.

A. ECG Signal Preprocessing

The preprocessing of raw ECG signals is necessary to reduce various types of noise that can be present in ECG signals, in order to improve the signal-to-noise ratio (SNR), which can be beneficial to the subsequent fiducial point (e.g., the location of QRS complex) detection and heartbeat classification. Typical sources of noise degrading ECG signals include power-line interference, baseline wander, artifacts due to muscle contraction, and electrode movement [21].

In this study, the preprocessing of ECG signals follows the previous literature and consists of baseline wander correction and band-pass filtering. The raw ECG signal was first processed to correct the baseline wander using a wavelets-based approach [22]. Following [23], the signal was band-pass filtered at 5–12 Hz to maximize the energy of QRS complex, removing high-frequency and low-frequency artifacts. The filtered signals were used in subsequent processing.

B. Heartbeat Segmentation

One heart cycle of ECG signal typically consists of three basic waveform components, namely, P wave, QRS complex, and T wave. The complete segmentation of ECG signal usually requires the accurate detection of boundaries and peak locations of the three waves, termed as fiducial points. The provided annotations of R-peak locations from the database were utilized to obtain heartbeat segments. The manual annotations were also utilized in the reference work [6]–[17], allowing us to directly compare our results and focus on measuring the performance of the novel proposed heartbeat classification method.

In real applications, the automatic R peak detection is required to fully automate the proposed heartbeat classification method. The incorporation of the automatic R peak detector might slightly degrade performance from two aspects. First, missed and erroneous detected heartbeats cannot be correctly classified. However, the heartbeat detection is a well-investigated problem and a number of existing schemes [24]–[26] are capable of detecting heartbeat with less than 0.5% error rate, on the MIT-BIH arrhythmia database. Second, the RR interval features will be deteriorated to some extent by the error caused by the R peak detector. In order to assess the impact of this type of error, an additional experiment is conducted by introducing a Gaussian-distributed artificial jitter (with zero mean and certain variance) to the annotated QRS locations. The performance will be presented and discussed in Section IV.

Given the sampling rate of 360 Hz, each heartbeat segment consists of 100 samples before the R peak location as the pre-R segment, and 200 samples after the R peak as the pro-R segment, i.e., a total of 300 samples corresponding to 0.83 s. The segment size is selected to include most, if not all, of the information in one heart cycle. In addition, the ratio of lengths of the pre-R segment and the pro-R segment is designed to be commensurate with that of typical lengths of the PR interval and the QT interval. The advantage of using a fixed heartbeat segment size lies in that it can avoid the detection of the fiducial points related with other waveform components (e.g., P wave and T wave), which usually are more sensitive to noise, due to their relatively lower magnitudes.

The limitation of using a fixed heartbeat segment size comes from that, in the case where the heart is beating much faster, the interval between two consecutive beats is shortened and the heartbeat segment may then contain information from neighboring beats, which could potentially result in the increase of false alarms of such an arrhythmia detector. For instance, heart rate changes can occur when the subject is doing intense exercise (e.g., running), or the subject is from a certain population (e.g., infants). In future study, we will investigate the effects of adapting heartbeat segment size to heart rhythm.

C. Wavelet Transform

Biomedical signals usually exhibit statistical characteristics that change over time or position. Due to this nonstationary nature, classical Fourier transform (FT) is unsatisfactory for the analysis as the FT provides a global characterization of the heartbeats frequency content. In contrast, wavelet transform (WT) provides a characterization in both temporal and frequency domains. This time-frequency analysis capability allows WT to be effective in analyzing nonstationary signals, such as ECG signals [27]. WT has been utilized in ECG signal processing for different purposes, including denoising [22], heartbeat detection [26], and feature extraction [7].

In our paper, WT is used as a feature extraction method. Daubechies wavelets of order 8 were selected due to their similarity with most characteristic QRS waveform. Given the sampling frequency of 360 Hz, the highest possible frequency presented is 180 Hz. It has been found that the energy of ECG signals is concentrated in the frequency range of 0.5–40 Hz [28]. After applying the four-level wavelet decomposition, this frequency range corresponds to the detail coefficients at level 3 (i.e.,

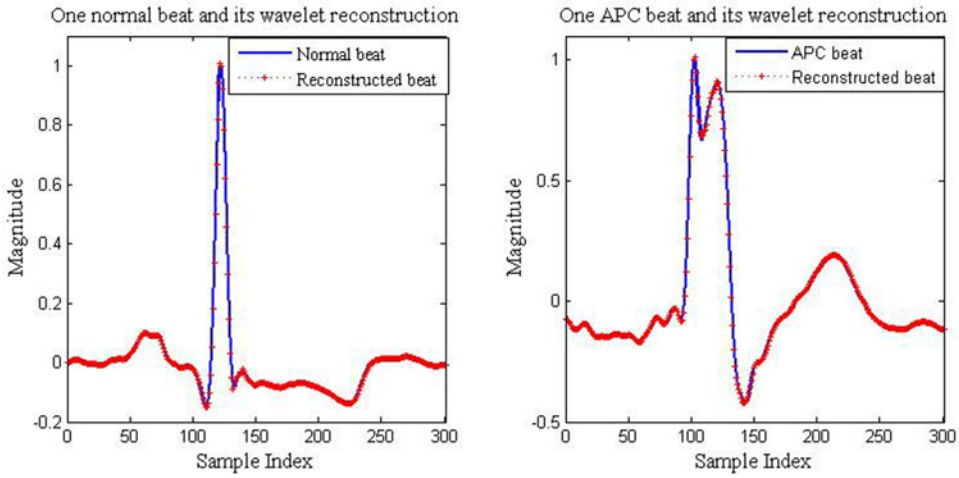

Fig. 3. Two example heartbeats and their respective wavelet reconstructed signals based on the extracted wavelet coefficients D3, D4, and A4.

D3) and 4 (i.e., D4) as well as the approximation coefficients at level 4 (i.e., A4). The dyadic decimation (down-sampling) is used and only the even indexed elements are kept, yielding the discrete WT (DWT). These 114 coefficients (32 from A4, 32 from D4, and 50 from D3) are thus extracted as the wavelet features for each heartbeat.

In Fig. 3, two example heartbeats (i.e., one normal beat and the other APC beat) are shown, along with their respective reconstructed signals based on the extracted coefficients D3, D4, and A4. It seems that the reconstructed signals almost coincide with original heartbeat, indicating that these wavelet features contain most of the energy of the original heartbeat, providing a good representation of temporal waveform and frequency characteristics of the given heartbeat.

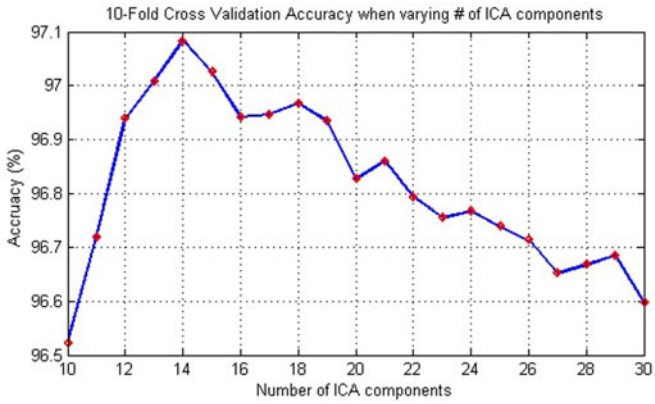

Fig. 4. Tenfold cross validation for selection of the number of ICs.

D. Independent Component Analysis

Independent component analysis (ICA) was originally proposed to solve the blind source separation (BSS) problem, the goal of which is to recover independent source signals from a set of observed signals, given little prior information [29]. ICA has been utilized in ECG signal analysis for blind source separation [30] and feature extraction [11].

ICA assumes that, at time instant t, the N observed signals $x_1(t), \ldots, x_N(t)$ are modeled as a linear combination of M underlying independent source signals $s_1(t), \ldots, s_M(t)$, termed as ICA components. Hence, ICA can be formulated in vector-matrix notation as

$$\mathbf{x}(t) = \mathbf{A} \cdot \mathbf{s}(t) \tag{1}$$

where $\mathbf{x}(t) = [x_1(t), \ldots, x_N(t)]^T$, $\mathbf{s}(t) = [s_1(t), \ldots, s_M(t)]^T$ and the matrix $\mathbf{A}$ is referred as the mixture matrix. ICA aims to estimate both $\mathbf{s}(t)$ and $\mathbf{A}$, assuming that the underlying source signals $s_1(t), \ldots, s_M(t)$ are statistically independent and non-Gaussianly distributed. The independent components are estimated by maximizing a certain quantitative metric of the statistical independence, such as kurtosis and negentropy [29].

In this study, ICA is employed as one of the tools for feature extraction. The implementation of a fast fixed-point algorithm [31] was used to estimate underlying independent components (ICs). In order to compute ICs from the predefined training set, five sample beats were randomly selected out of every class in each recording (if the actual number is less than five, then all the beats were used). As such, a total of 626 beats covering all of 16 classes were obtained from the training dataset for estimating the ICs. The trained ICs are applied to both the training and test dataset so that 14 ICA coefficients are derived as features for each heartbeat. In order to study the effect of the number of ICs on heartbeat classification and select the "optimum" number of ICs, tenfold cross validation was evaluated on the training dataset, varying the number of ICs from 10 to 30; only the resulting ICA coefficients are used as features of heartbeats fed into SVM classifier. Since the fast ICA algorithm uses a random initialization, the calculated ICs depend on the initialization. Thus, the process is repeated for five iterations and the average performance is reported. The results are shown in Fig. 4; as we can see, the average cross validation accuracy tends to increase when the number of ICs increases from 10 to 14 and decreases afterward. Hence, 14 seems to be a good choice of the number of ICs. Therefore, 14 ICs were trained using the predefined training dataset, containing approximate 95% of the sum of nonzero eigenvalues of the estimated

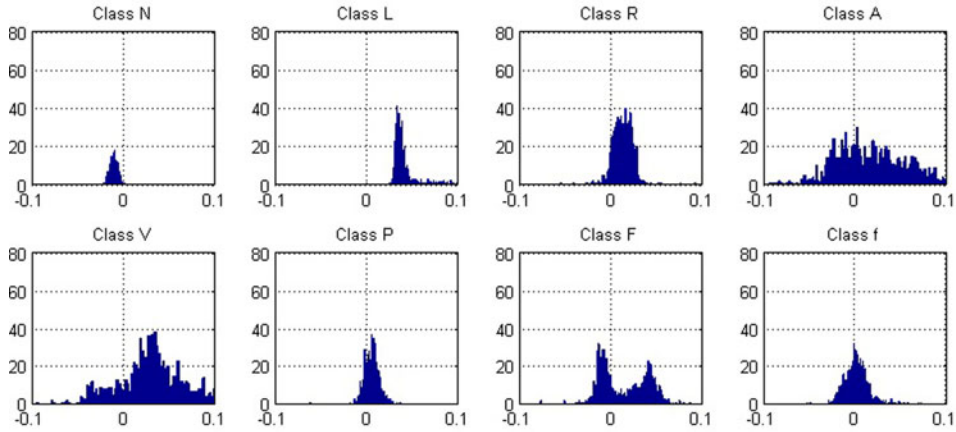

Fig. 5. Histograms of the second ICA feature of eight heartbeat classes, including the normal and other seven arrhythmias classes; approximately 1000 heartbeats from each of eight classes were used to compute the histogram. (The number of beats from the other eight classes are much smaller than 1000; we did not show the histograms of the other eight classes to avoid unfair comparison.)

covariance matrix. Finally, 14 ICA coefficients are extracted as the ICA features for each heartbeat. The resulting 14 ICA features can be understood as "coordinates," determining the "location" of heartbeat data in the corresponding feature space.

Fig. 5 shows the histograms of the second ICA feature (i.e., the weight on the second IC) from the normal heartbeat class and seven arrhythmia classes (approximately 1000 heartbeats from each of eight classes are used to calculate the corresponding histogram). As we can see, the distributions of the selected ICA coefficient vary significantly between different classes, indicating that this ICA feature is good at distinguishing these eight classes. The behavior is also repeated similarly for the other ICA coefficients and classes.

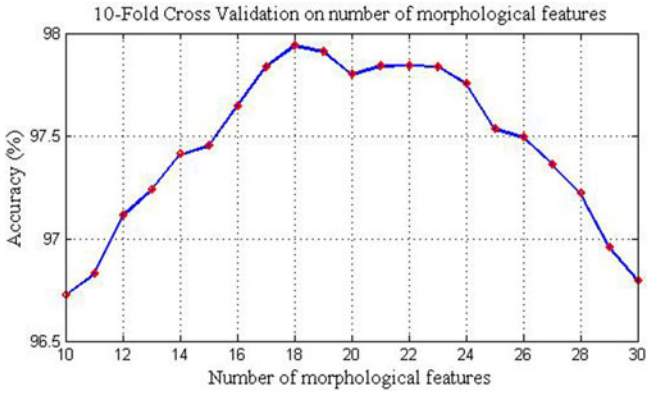

Fig. 6. Tenfold cross validation for selection of the number of morphological features.

E. Principal Component Analysis

One-hundred and fourteen wavelets features and 14 ICA features have been obtained for each heartbeat, referred as the "morphological features," providing the characterization of waveform shape of the heartbeat. These two types of features are first concatenated and PCA is applied to reduce the feature dimensionality. The tenfold cross validation was performed on the lead A signals of the selected training dataset, in order to select dimensionality of the final morphological features, as depicted in Fig. 6. Eighteen principal components are obtained based on the training dataset are selected corresponding to retaining approximately 90% of the variance in the training dataset. Finally, 18 morphological features are derived accordingly for the representation of each heartbeat. PCA is introduced before the concatenation of morphological and dynamic features since these two sets of features focus on different characteristics (i.e., inside the heartbeat and between the heartbeats). On the other hand, feature dimension reduction is applied to morphological features in order to balance the importance of the two types of features, since unbalanced numbers of morphological and dynamic features could bias SVM classifier, leading to degraded classification performance.

F. RR Interval Features

Besides morphological features, RR interval features are computed for characterizing the dynamic information of the heartbeat, termed as "dynamic" features. Four RR features are derived to represent the rhythm of the heartbeat at various scales, namely, previous RR, post RR, local RR, and average RR interval features.

The previous RR feature is calculated as the interval between a given R peak and its previous R peak, and the post RR feature as that of the current R peak and the following one. They are combined to provide instantaneous rhythm information of the heartbeat. The local RR interval is computed by averaging all the RR intervals within a sliding window covering the past 10-s episode of the given heartbeat; hence the local RR feature characterizes the average rhythm in the past 10-s local duration. Similarly, the average RR interval is obtained as the average of RR intervals within a sliding window covering the past 5-min episode of the heartbeat, reflecting the background rhythm information in the past 5-min episode.

It is worth noting that the local RR and the average RR are different from that used in [8], [12], [17], in which the local RR feature was calculated as the average of RR intervals of

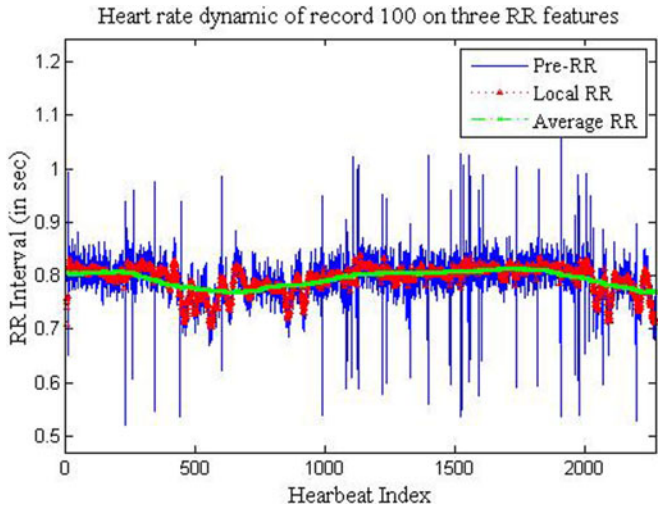

Fig. 7. Previous RR, local RR, and average RR features of the heartbeats from the record 100 in MIT database, plotted sequentially over time.

ten heartbeats centered at the given beat, and the average RR feature was obtained by averaging RR intervals of the all heartbeats from the same record, making this feature identical for every single heartbeat in the same ECG recording. Such an estimate of the average RR feature is not only unrealistic in a real-time application, but also a biased estimate of background dynamic information. In our paper, the local RR and the average RR features are adapted as the average of RR intervals within the corresponding past episodes of the given heartbeat, so that more realistic estimates are obtained regarding the local and the background dynamic information of heartbeat and the real-time feature extraction is ensured.

Fig. 7 shows three RR interval features, i.e., the previous RR, local RR, and average RR features, of the heartbeats from the record 100 in MIT database, plotted sequentially over time. This serves as an illustration that how the three RR interval features reflects the rhythm information at different scales.

G. Support Vector Machine

In this study, an SVM classifier is considered for classifying heartbeats into one of the 16 classes or the 5 classes. The SVM, proposed by Vapnik [32], basically consists of building an optimal hyperplane that maximizes the separation margin between two different classes. This margin-based approach typically constructs classification models with excellent generalization ability, making it a powerful tool in various applications [33].

For a two-class classification problem, let the training set consists of N examples $\{(\mathbf{x}_i, y_i), i = 1, \ldots, N\}$, where $\mathbf{x}_i \in \Re^d$ denotes the d-dimensional feature vector of the ith example and the $y_i \in \Re$ denotes its class label, $y_i \in \{\pm 1\}$. The problem is to construct a decision function $f(\mathbf{x})$ based on the training set that can be used to predict the output class label of future test example based on its input feature vector. Following [34], it can be formulated as an optimal problem, and the resultant decision function is given as

$$f(\mathbf{x}) = \text{sign}\left(\sum_{i \in SV\,s} \alpha_i y_i K(\mathbf{x}_i, \mathbf{x}) + b\right) \tag{2}$$

where the function $K(.,.)$ is the kernel function that map the data into a higher dimensional space. α_i is the Lagrange multiplier for each training data sample and usually only a few α_i are nonzero. Those training examples whose α_i are nonzero, are termed as support vectors (SVs). The final decision function $f(x)$ is actually only determined by these few SVs.

Support vector machines are intrinsically binary classifiers. A number of multiclass classification strategies have been developed to extend SVM to address multiclass classification problem [34], such as heartbeat classification problem. The most popular approaches include the one-against-all (OAA) and the one-against-one (OAO) methods, essentially decomposing the multiclass problem into a set of binary classification problem [35].

In addition to the predicted labels, probabilistic estimates can also be obtained for each prediction following [36]. Given K-class data, for any input feature vector $\mathbf{x}$, the probability of $\mathbf{x}$ being from the ith class is denoted as

$$p_i = P(y = i \,|\, \mathbf{x}). \tag{3}$$

In the OAO approach, the classifier provides pairwise class probabilities given by

$$r_{ij} = P(y = i \text{ or } j, \mathbf{x}). \tag{4}$$

The pairwise posterior probabilities can be estimated approximately using a sigmoid function as follows:

$$r_{ij} = \frac{1}{1 + \exp(A\hat{f} + B)} \tag{5}$$

where $\hat{f}$ is the decision value (i.e., output of the decision function) at $\mathbf{x}$; A and B are estimated by maximizing the log likelihood of the training data using their labels and decision values.

In this paper, the SVM with the radial basis function (RBF) kernel is used. First, the model parameters (i.e., the regularization parameter C of the SVM and the width parameter σ of the kernel) were selected using the tenfold cross validation on the training dataset (as defined in Section II). Following the model parameter selection, the SVM classifier was trained using the training dataset. In the classification phase, the resulting SVM classifier was used to predict class labels as well as the probability estimates of the heartbeats from the testing dataset. All SVM algorithms are implemented using the LIBSVM [37] package.

H. Two-Lead Fusion

Each heartbeat segment consists of two signals derived from the lead A and lead B. These two signals can be treated as two observations on the same cardiac activity from two different positions. The information from the two signals can be fused to make the final decision, so that the classification confidence is enhanced.

The same procedure was independently applied to the two signals, including feature extraction and classification. Two

individual SVM classifiers were trained separately using the lead A and the lead B signals of heartbeats from the training dataset. The two classifiers are applied, respectively, to the lead A and the lead B signals of each test heartbeat, so that two independent answers are derived from the two classifiers for each heartbeat, which are combined to make the final decision on the beat category.

Two different approaches are adopted to combine the two independent answers from the individual classifiers. The first method, termed as *rejection approach*, is simply to compare the independent classification answers from the two individual classifiers. Ideally, the two answers should be the same for a given heartbeat. In the case that an inconsistency occurs, at least one of the two classification results is incorrect, which can possibly be caused by the loss of quality for the signal from the corresponding lead, perhaps due to artifacts caused by muscle movement, electrode contraction, etc. In such circumstances, the inconsistency can be resolved simply by rejecting the heartbeat, i.e., no final decision is made. The price paid for this *rejection approach* is that no decision is made for a small portion of heartbeats. The rejected heartbeat can possibly be reserved for later manually review by physicians.

The second approach, namely, *Bayesian approach*, incorporates the probability estimates from the two individual classifiers to make the final decision. Given K-class data, assuming that the outputs from two classifiers to be combined, the final probability estimates $\bar{P}(y = i \,|\, \{\mathbf{x}_1, \mathbf{x}_2\})$ can be calculated based on individual probabilities $P_l(y = i \,|\, \mathbf{x}_l)$, $l = 1, 2$, that are obtained from the corresponding individual (i.e., single-lead) classifier, using a Bayesian product approach, as follows:

$$\bar{P}(y = i \,|\, \{\mathbf{x}_1, \mathbf{x}_2\}) = \frac{\prod_{l=1}^{2} P_l(y = i \,|\, \mathbf{x}_l)}{\sum_{j=1}^{K} \prod_{l=1}^{2} P_l(y = j \,|\, \mathbf{x}_l)} \tag{6}$$

where $\mathbf{x}_l$ is the feature representation of the heartbeat on the lth lead, feeding into the lth individual classifier, $l = 1, 2$. Hence, the probability of the heartbeat being from the ith class is given as the joint probability of the lead A signal and the lead B signal being from the ith class; the joint probability is normalized into the range of $[0, 1]$ to be a valid probability estimate. Finally, the winning class k is determined to correspond to the highest final probability estimate in M classes, given by

$$k = \underset{i}{\operatorname{argmax}}\, \bar{P}(y = i \,|\, \{\mathbf{x}_1, \mathbf{x}_2\}). \tag{7}$$

IV. Results

A. Class-Oriented Evaluation

In the "class-oriented" evaluation, two individual classifiers were trained separately using the lead A signals and the lead B signals of the training dataset defined in Section II. The trained individual classifiers were utilized to predict the lead A signal and the lead B signal of each test heartbeat, respectively. Based on the lead A signals, 84908 heartbeats were correctly classified out of 86009 test beats with an accuracy of 98.72%. Using the lead B signals, the heartbeat classification performance got slightly worse, with 84805 heartbeats being correctly recognized, corresponding to an accuracy of 98.60%.

As discussed in Section III-H, the two fusion approaches, namely, the *rejection approach* and the *Bayesian approach* were investigated to combine the two classification results from both lead signals to make the final decision for each heartbeat. The *rejection approach* resulted in an accuracy of 99.71% with a price of rejecting 2054 heartbeats (i.e., set aside for physician review). The *Bayesian approach*, based on the fusion of probability estimates, yielded an average accuracy of 99.32%. Both approaches show significant improvement in performance over that using individual lead signals. The *rejection approach* yielded a slightly better performance, at the price of rejecting a small portion of heartbeats. The performance on each individual heartbeat class is evaluated using two metrics, namely, the sensitivity (Se) and positive predictivity (+P), which are calculated based on the number of true positive (TP), false negative (FN), and false positive (FP), as follows:

$$\text{Se} = \frac{\text{TP}}{\text{TP} + \text{FN}} \tag{8}$$

$$+\text{P} = \frac{\text{TP}}{\text{TP} + \text{FP}} \tag{9}$$

where TP is defined as the instance from the given class correctly classified as from that class; FN is given as the instances from the given class (any of the 16 classes or the 5 classes) being incorrectly classified as from other classes; FP is defined as the instance from the other class incorrectly classified as from the given class. The sensitivity and positive predictivity of each individual class are summarized in Table IV. As we can see, the both approaches exhibited reasonable individual-class performances, showing good sensitivity and positive predictivity, except on a few small heartbeat classes, e.g., "e" and "Q." The final confusion matrices for using the two fusion approaches are presented in Fig. 8.

Table V provides a comparison of classification accuracies between the proposed approach and earlier published results [6], [7], [9]–[11], [16], based on the "class-oriented" evaluation scheme. We observe that the proposed approach obtained improvement in heartbeat classification accuracy over the literature paper. The improved results indicate that the proposed feature representation of heartbeats, based on a combination of morphological and dynamic features, exhibits a superior performance for discriminating heartbeat segments from a variety of heartbeat classes. In addition, the proposed two-lead fusion strategy enhances the classification confidence and improves the heartbeat classification performance. Based on these results, we can conclude that the proposed method offers improvement over earlier approaches.

Regarding the contribution of different types of features, by using wavelets and ICA features alone, the resulting average classification accuracy is 95.32% and 94.25%, respectively. By using WT and ICA features together (with PCA), the resulting classification accuracy is 98.46%. By adding RR features, the resulting classification accuracy improves to 99.32%.

Finally, we need to note that the "class-oriented" evaluation is not a realistic measure of classifier performance in real

TABLE IV
PERFORMANCE SUMMARY ON EACH INDIVIDUAL CLASS IN THE "CLASS-ORIENTED" EVALUATION

Heartbeat Class	Train Num.	Test Num.	Rn Method I	TP Method I	Se (%) Method I	+P (%) Method I	TP Method II	Se (%) Method II	+P (%) Method II
NOR ('**N**')	9753	65264	1222	63949	99.85	99.85	64978	99.56	99.71
LBBB ('**L**')	3229	4843	45	4798	100	99.85	4838	99.90	99.65
RBBB ('**R**')	2902	4353	52	4292	99.79	100	4340	99.70	99.95
APC ('**A**')	1019	1527	166	1315	96.62	96.62	1435	93.98	91.87
PVC ('**V**')	2852	4277	350	3899	99.29	98.96	4203	98.27	97.20
PACE ('**P**')	2810	4214	22	4192	100	99.98	4208	99.86	99.93
AP ('**a**')	75	75	27	43	89.58	91.49	60	80.00	85.71
VF ('**!**')	236	236	32	203	99.51	98.54	231	97.88	88.85
VFN ('**F**')	401	401	54	326	93.95	96.17	365	91.02	89.46
BAP ('**x**')	97	96	18	77	98.72	100	86	89.58	100
NE ('**j**')	115	114	17	90	92.78	92.78	101	88.60	82.79
FPN ('**f**')	491	491	34	453	99.12	98.91	481	97.96	97.57
VE ('**E**')	53	53	0	52	98.11	100	53	100	100
NP ('**J**')	42	41	6	33	94.29	97.06	38	92.68	90.48
AE ('**e**')	8	8	3	3	60	100	5	62.50	62.50
UN ('**Q**')	17	16	6	4	40	100	5	31.25	71.43
Total	24100	86009	2054	83712	99.71	99.71	85424	99.32	99.32

The table includes the following information (from left to right): heartbeat class, number of training beats, number of testing beats; number of rejected beats (Rn), true positive (TP), sensitivity (Se), positive predictivity (+P) when the *rejection fusion approach* is utilized; Rn, TP, Se, +P when the *Bayesian fusion approach* is utilized.

Predicted Labels / **Ground Truth Labels**

	N	L	R	A	V	P	a	!	F	x	j	f	E	J	e	Q	Σ
N	**63949**	4	0	45	23	0	3	0	9	0	7	2	0	0	0	0	**64042**
L	0	**4798**	0	0	0	0	0	0	0	0	0	0	0	0	0	0	**4798**
R	9	0	**4292**	0	0	0	0	0	0	0	0	0	0	0	0	0	**4301**
A	44	1	0	**1315**	0	0	1	0	0	0	0	0	0	0	0	0	**1361**
V	21	1	0	0	**3899**	0	0	3	3	0	0	0	0	0	0	0	**3927**
P	0	0	0	0	0	**4192**	0	0	0	0	0	0	0	0	0	0	**4192**
a	3	0	0	0	2	0	**43**	0	0	0	0	0	0	0	0	0	**48**
!	0	0	0	0	1	0	0	**203**	0	0	0	0	0	0	0	0	**204**
F	7	0	0	0	14	0	0	0	**326**	0	0	0	0	0	0	0	**347**
x	1	0	0	0	0	0	0	0	0	**77**	0	0	0	0	0	0	**78**
j	4	0	0	1	0	0	0	0	1	0	**90**	0	0	1	0	0	**97**
f	2	1	0	0	0	1	0	0	0	0	0	**453**	0	0	0	0	**457**
E	1	0	0	0	0	0	0	0	0	0	0	0	**52**	0	0	0	**53**
J	2	0	0	0	0	0	0	0	0	0	0	0	0	**33**	0	0	**35**
e	2	0	0	0	0	0	0	0	0	0	0	0	0	0	**3**	0	**5**
Q	2	0	0	0	1	0	0	0	0	0	0	3	0	0	0	**4**	**10**
Σ	**64047**	**4805**	**4292**	**1361**	**3940**	**4193**	**47**	**206**	**339**	**77**	**97**	**458**	**52**	**34**	**3**	**4**	**83955**

(a)

Predicted Labels / **Ground Truth Labels**

	N	L	R	A	V	P	a	!	F	x	j	f	E	J	e	Q	Σ
N	**64978**	6	0	118	84	0	6	13	31	0	21	4	0	0	2	1	**65264**
L	4	**4838**	0	0	1	0	0	0	0	0	0	0	0	0	0	0	**4843**
R	6	0	**4340**	4	2	0	0	0	0	0	0	0	0	1	0	0	**4353**
A	75	4	2	**1435**	5	0	3	0	2	0	0	0	0	0	1	0	**1527**
V	44	3	0	1	**4203**	0	1	14	10	0	0	1	0	0	0	0	**4277**
P	0	3	0	0	0	**4208**	0	0	0	0	0	3	0	0	0	0	**4214**
a	10	0	0	1	4	0	**60**	0	0	0	0	0	0	0	0	0	**75**
!	2	0	0	0	3	0	0	**231**	0	0	0	0	0	0	0	0	**236**
F	15	0	0	0	19	0	0	0	**365**	0	0	0	0	2	0	0	**401**
x	7	0	0	1	0	0	0	2	0	**86**	0	0	0	0	0	0	**96**
j	11	0	0	1	0	0	0	0	0	0	**101**	0	0	1	0	0	**114**
f	5	1	0	0	0	3	0	0	0	0	0	**481**	0	0	0	1	**491**
E	0	0	0	0	0	0	0	0	0	0	0	0	**53**	0	0	0	**53**
J	2	0	0	1	0	0	0	0	0	0	0	0	0	**38**	0	0	**41**
e	3	0	0	0	0	0	0	0	0	0	0	0	0	0	**5**	0	**8**
Q	4	0	0	0	3	0	0	0	0	0	0	4	0	0	0	**5**	**16**
Σ	**65166**	**4855**	**4342**	**1562**	**4324**	**4211**	**70**	**260**	**408**	**86**	**122**	**493**	**53**	**42**	**8**	**7**	**86009**

(b)

Fig. 8. Final confusion matrices of using the two fusion approaches. (a) Final confusion matrix using the *rejection fusion approach*. (b) Final confusion matrix using the *Bayesian fusion approach*.

TABLE V
COMPARISON OF CLASSIFICATION ACCURACIES BETWEEN THE PROPOSED METHOD AND THE REFERENCE WORK [6], [7], [9]–[11], [16], USING THE BIASED CLASS-ORIENTED VALIDATION

Reference	Features	Accuracy (%)
Lagerholm[6]	Hermite	98.49
Prasad[7]	Wavelet + RR	96.77
Osowski[9]	HOS + Hermite	98.18
Rodriguez[10]	Waveform	96.13
Jiang[11]	Wavelet + ICA	98.86
Oliveira[16]	Waveform + RR	98
Proposed Method	**Wavelet + ICA + RR**	**99.32(99.71)**

applications. It provides a quantification of capability of the classifier and features for separation among different beat classes when they are perfectly modeled. This evaluation is conducted in order to make a comparison with previous works.

B. Subject-Oriented Evaluation

Besides the "class-oriented" evaluation, the "subject-oriented" evaluation is employed to estimate the performance of the proposed method in practice. As discussed in Section II-B, the same database division is adopted as in the literature [8], [15], [17], i.e., the 22 records used as the training set and the other 22 records as the testing set. The results are reported in the ANSI/AAMI defined five-class division; the average performance is shown in Table VI. In addition, the record-by-record cross validation is performed. For each record, the model is trained on the data from the other 43 records and is subsequently used to test the heartbeats of the given record; the procedure is repeated for all 44 records. The performance is averaged and presented in Table VI. The confusion matrices of the two above-mentioned tests are shown in Tables VII and VIII, respectively.

We compare the observed results with the results in [8], [15], and [17] based on the following metrics, namely, classification accuracy, Se and +P of the supraventricular ectopic class (the class "S"), as well as that of the ventricular ectopic class (the class "V"). The comparison is presented in Table VI. As we can observe, the proposed method yielded comparable performances, in terms of general accuracy, as well as on the class "S" and class "V." The worse performance on the class "S" can possibly be attributed to fewer data samples of class "S" than class "V." As expected, the performance of the "subject-oriented" evaluation shows worse results than that of the "class-oriented" evaluation, due to interindividual variability in physiological characteristics.

TABLE VI
COMPARISON OF "SUBJECT-ORIENTED" EVALUATION RESULTS BETWEEN THE PROPOSED METHOD AND THE REFERENCE WORKS [8], [15]

Metric	De Chazal [8]	Llamedo [15]	**Proposed Method**	**Proposed Method CV[a]**
Accuracy (%)	81.9	93	**86.4**	**88.2**
Se of class 'S' (%)	75.9	77	**60.8**	**56.4**
+P of class 'S' (%)	38.5	39	**52.3**	**55.2**
Se of class 'V' (%)	77.7	81	**81.5**	**84.7**
+P of class 'V' (%)	81.9	87	**63.1**	**60.3**

[a] Cross Validation

TABLE VII
CONFUSION MATRIX USING THE SUBJECT-ORIENTED TEST

		Predicted Label				
		n	s	v	f	q
Reference	N	39157	931	1284	2816	50
	S	502	1199	252	12	7
	V	284	160	2624	139	13
	F	199	1	110	76	2
	Q	2	0	5	0	0

TABLE VIII
CONFUSION MATRIX OF CROSS-VALIDATION USING THE SUBJECT-ORIENTED TEST

		Predicted Label				
		n	s	v	f	q
Reference	N	81068	1079	3631	4217	88
	S	733	1677	536	19	7
	V	429	281	6335	407	28
	F	361	2	147	287	5
	Q	5	2	7	1	0

C. Feature Extraction Robustness Test

As discussed in Section III-B, in real applications, the automatic QRS detection should be incorporated to fully automate the proposed heartbeat classification method. The automatic R peak detection can introduce error in RR interval features, as well as the computation of other features, since there could exist a shift between the actual and the detected R peak locations. In order to test the robustness of the proposed feature extraction method, one experiment is conducted by introducing a Gaussian-distributed artificial jitter (with zero mean and a standard deviation of five samples) to the annotated QRS locations. The "five-sample" is a typical amount of shift introduced by the QRS detector. It yielded a general accuracy of 99.01% (99.28% with 3.2% rejections), based on the "class-oriented" evaluation, compared with the original performance of 99.32% (99.71% with 2.4% rejections), using the actual annotated R peak locations. This serves as a proof of the robustness of the proposed feature extraction methodology.

V. CONCLUSION

In this paper, we presented a systematic approach for automatic heartbeat classification. One novel feature representation of heartbeat segments is proposed, based on a combination of a set of derived morphological and dynamic features. Improved wavelets, ICA and RR interval features are utilized. The classification is finally done using 18 PCA projection coefficients computed from the concatenated wavelet and ICA features, plus four RR interval features. Besides, two fusion approaches are developed to fuse the information of both lead signals to make the classification decision, using the probability estimates given by SVM classifiers. On the benchmark MIT-BIH arrhythmia database, the proposed method yields an accuracy of 99.3% (99.7% with 2.4% rejections) in the "class-oriented" evaluation and an accuracy of 86.4% in the "subject-oriented" evaluation. The results of "class-oriented" evaluation can be interpreted as a measurement of performance achievable if the classifier could be trained using the beats from the patients to be analyzed. The results of the "subject-oriented" evaluation can be deemed as a more realistic estimate of potential performance of the proposed method in real applications.

In the future, it is of interest to investigate certain automatic patient customization scheme, allowing the proposed heartbeat classification method being capable of adapting to individual physiological characteristics. In addition, it is interesting to explore potential benefits of adapting heartbeat segmentation to heart rhythm, avoiding the increase of false alarms caused by wild heart rhythm variability in some scenarios, or for certain population.

REFERENCES

[1] K. Robert and E.C. Colleen, *Basis and Treatment of Cardiac Arrhythmias*, 1st ed. New York: Springer-Verlag, 2006.
[2] V. X. Alfonso and J. Tompkins, "Detecting ventricular fibrillation," *IEEE Trans. Biomed. Eng.*, vol. 54, no. 1, pp. 174–177, Jan. 2007.
[3] S. Barro, R. Ruiz, D. Cabello, and J. Mira, "Algorithmic sequential decision-making in the frequency domain for life threatening ventricular arrhythmias and imitative artefacts: A diagnostic system," *IEEE Trans. Biomed. Eng.*, vol. 11, no. 4, pp. 320–328, Jul. 1989.
[4] K. Minami, H. Nakajima, and T. Toyoshima, "Real-time discrimination of ventricular tachyarrhythmia with Fourier-transform neural network," *IEEE Trans. Biomed. Eng.*, vol. 46, no. 2, pp. 179–185, Feb. 1999.
[5] J. A. Kastor, *Arrhythmias*, 2nd ed. London: W.B. Saunders, 1994.
[6] M. Lagerholm, C. Peterson, G. Braccini, L. Edenbrandt, and L. Sornmo, "Clustering ECG complexes using Hermite functions and self-organizing maps," *IEEE Trans. Biomed. Eng.*, vol. 47, no. 7, pp. 838–848, Jul. 2000.
[7] G. K. Prasad and J. S. Sahambi, "Classification of ECG arrhythmias using multi-resolution analysis and neural networks," in *Proc. Conf. Convergent Technol. Asia-Pacific Region*, Oct. 2003, pp. 227–231.
[8] P. de Chazal, M. O. Dwyer, and R. B. Reilly, "Automatic classification of heartbeats using ECG morphology and heartbeat interval features," *IEEE Trans. Biomed. Eng.*, vol. 51, no. 7, pp. 1196–1206, Jul. 2004.
[9] S. Osowski, L. T. Hoa, and T. Markiewic, "Support vector machine-based expert system for reliable heartbeat recognition," *IEEE Trans. Biomed. Eng.*, vol. 51, no. 4, pp. 582–589, Apr. 2004.
[10] J. Rodriguez, A. Goni, and A. Illarramendi, "Real-time classification of ECGs on a PDA," *IEEE Trans. Info. Tech. Biomed.*, vol. 9, no. 1, pp. 23–34, Mar. 2005.

[11] X. Jiang, L. Q Zhang, Q. B. Zhao, and S. Albayrak, "ECG arrhythmias recognition system based on independent component analysis feature extraction," in *Proc. IEEE Region 10 Conf.*, Nov. 2006, pp. 1–4.

[12] P. de Chazal and R. B. Reilly, "A patient-adapting heartbeat classifier using ECG morphology and heartbeat interval features," *IEEE Trans. Biomed. Eng.*, vol. 53, no. 12, pp. 2535–2543, Dec. 2006.

[13] W. Jiang and G. S. Kong, "Block-based neural networks for personalized ecg signal classification," *IEEE Trans. Neural Networks*, vol. 18, no. 6, pp. 1750–1761, Nov. 2007.

[14] T. Ince, S. Kiranyaz, and M. Gabbouj, "A generic and robust system for automated patient-specific classification of ECG signals," *IEEE Trans. Biomed. Eng.*, vol. 56, no. 5, pp. 1415–1426, May 2009.

[15] M. Llamedo and J. P. Martinez, "Heartbeat classification using feature selection driven by database generalization criteria," *IEEE Trans. Biomed. Eng.*, vol. 58, no. 3, pp. 616–625, Mar. 2011.

[16] L. de Oliveira, R. Andreao, and M. Sarcinelli, "Premature Ventricular beat classification using a dynamic Bayesian network," in *Proc. IEEE Int. Conf. Eng. Med. Biol. Soc.*, Aug./Sep. 2011, pp. 4984–4987.

[17] G. de Lannoy, D. Francois, J. Delbeke, and M. Verleysen, "Weighted conditional random fields for supervised interpatient heartbeat classification," *IEEE Trans. Biomed. Eng.*, vol. 59, no. 1, pp. 241–247, Jan. 2012.

[18] MIT-BIH Arrhythmias Database. [Online]. Available: http://www.physionet.org/physiobank/database/mitdb/.

[19] *Testing and Reporting Performance Results of Cardiac Rhythm and ST Segment Measurement Algorithms*, ANSI/AAMI EC57:1998 standard, Association for the Advancement of Medical Instrumentation, 1998.

[20] C. Ye, M. Coimbra, and B. V. K. Vijaya Kumar, "Arrhythmia detection and classification using morphological and dynamic features of ECG signals," in *Proc. IEEE Int. Eng. Med. Biol. Soc.*, Aug./Sep. 2010, pp. 1918–1921.

[21] A. U. Rajendra and J. S. Suri, *Advances in Cardiac Signal Processing*, 1st ed. New York: Springer-Verlag, 2009.

[22] D. Zhang, "Wavelet approach for ECG baseline wander correction and noise reduction," in *Proc. IEEE Int. Eng. Med. Biol. Soc.*, 2005, pp. 1212–1215.

[23] J. Pan and W. J. Tompkins, "A real-time QRS detection algorithm," *IEEE Trans. Biomed. Eng.*, vol. 32, no. 3, pp. 230–236, Mar. 1985.

[24] P. Laguna, R. Jane, and P. Caminal, "Automatic detection of wave boundaries in multilead ECG signals: Validation with the CSE database," *Comput. Biomed. Res.*, vol. 27, no. 1, 1994.

[25] V. X. Afonso, W. J. Tompkins, T. Q. Nguyen, and L. Shen, "ECG beat detection using filter banks," *IEEE Trans. Biomed. Eng.*, vol. 46, no. 2, pp. 192–202, Feb. 1999.

[26] S. Kadambe, R. Murray, and G. F. Boudreaux, "Wavelet transform-based QRS complex detector," *IEEE Trans. Biomed. Eng.*, vol. 46, no. 7, pp. 838–848, Jul. 1999.

[27] S. Reddy, *Biomedical Signal Processing: Principles and Techniques*. New York: McGraw-Hill, 2005.

[28] N. V. Thakor, J. G. Webster, and W.J. Tompkins, "Estimation of QRS complex power spectra for design of a QRS filter," *IEEE Trans. Biomed. Eng.*, vol. 31, no. 11, pp. 702–706, Nov. 1984.

[29] A. Hyvrinen, J. Karhunen, and E. Oja, *Independent Component Analysis*. New York: Wiley-Interscience, 2001.

[30] J. J. Rieta, F. Castells, C. Sanchez, V. Zarzoso, and J. Millet, "Atrial activity extraction for atrial fibrillation analysis using blind source separation," *IEEE Trans. Biomed. Eng.*, vol. 51, no. 7, pp. 1176–1186, Jul. 2004.

[31] A. Hyvrinen, "Fast and robust fixed-point algorithms for independent component analysis," *IEEE Trans. Neural Network*, vol. 10, no. 3, pp. 626–634, May 1999.

[32] V. N. Vapnik, *The Nature of Statistical Learning Theory.*. New York: Springer-Verlag, 1995.

[33] H. Byun and S. W. Lee, "A survey of pattern recognition applications of support vector machines," *Int. J. Pattern Recognit. Artif. Intell.*, vol. 17, no. 3, pp. 459–486, 2003.

[34] C. Cortes and V. N. Vapnik, "Support vector networks," *J. Mach. Learn.*, vol. 20, pp. 1–25, 1995.

[35] C. W. Hsu and C. J. Lin, "A comparison of methods for multi-class support vector machines," *IEEE Trans. Neural. Net.*, vol. 13, no. 2, pp. 415–425, 2002.

[36] T. F. Wu, C. J. Lin, and R. C. Weng, "Probability estimates for multi-class classification by pairwise coupling," *J. Mach. Learn.*, vol. 5, pp. 975–1005, 2004.

[37] C. C. Chang and C. J. Lin. (2011). "LIBSVM: A library for support vector machines," *ACM Trans. Intell. Sys. and Tech.*, [Online]. *2*,pp. 27:1–27:27. Available: http://www.csie.ntu.edu.tw/cjlin/libsvm.

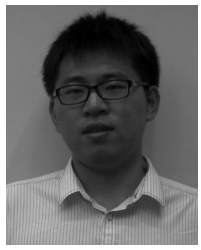

Can Ye (S'10) received the B.Eng. degree in information engineering from the Department of Information Science and Electronic Engineering, Zhejiang University, Zhejiang, China, in 2008. He is currently working toward the dual Ph.D. degrees at the Department of Electrical and Computer Engineering, Carnegie Mellon University, Pittsburgh, PA as well as at the Department of Computer Science, University of Porto, Porto, Portugal.

His research interests include signal processing and machine learning of physiological vital signals (such as ECG and blood pressure) for online monitoring and detection of abnormal health events, especially the identification of a variety of cardiac abnormalities through the analysis of ECG signals.

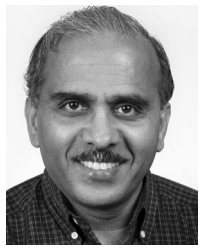

B. V. K. Vijaya Kumar (F'10) is currently a Professor of Electrical and Computer Engineering (ECE) and the Associate Dean for Graduate and Faculty Affairs of College of Engineering, at Carnegie Mellon University (CMU). He served as the Associate Department Head of the ECE Department from 1994 to 1996 and as the Acting Head of the ECE Department from 2004 to 2005. His research interests include pattern recognition, biometrics and coding and signal processing for data storage systems. His publications include the book entitled *Correlation Pattern Recognition* (coauthored with Dr. A. Mahalanobis and Dr. R. Juday, Cambridge University Press, November 2005), 15 book chapters, and more than 500 technical papers.

He served as a Pattern Recognition Topical Editor for the Information Processing Division of Applied Optics. He served as an Associate Editor for the IEEE TRANSACTIONS ON INFORMATION FORENSICS AND SECURITY from 2004 to 2009. He serves on many biometrics and data storage conference program committees and was the Co-General Chair of the 2004 Optical Data Storage conference, the Co-General Chair of the 2005 IEEE AutoID Workshop, the Co-Chair of the 2008, 2009, and 2010 SPIE conferences on Biometric Technology for Human Identification and is the Co-Chair of the 2012 Biometrics: Theory, Applications and Systems (BTAS) conference. He serves on the IEEE Biometric Council and was a Former Member of the IEEE Signal Processing Society's Technical Committee on Information Forensics and Security. In 2003, he received the Eta Kappa Nu Award for Excellence in Teaching in the ECE Department at CMU, the Carnegie Institute of Technologys Dowd Fellowship for educational contributions and in 2009 was a corecipient of the Carnegie Institute of Technologys Outstanding Faculty Research Award. He is a Fellow of the SPIE, the Optical Society of America (OSA), and the International Association of Pattern Recognition (IAPR).

Miguel Tavares Coimbra (M'06) received the B.Sc. degree in electrical engineering and computers from the Faculty of Engineering, University of Porto, Porto, Portugal. He started the PhD studies in 2000 at Kings College London, London, U.K., in the area of computer vision, he then transferred to Queen Mary, University of London, London, U.K., in 2002, where he received the Ph.D. degree in 2004.

He was a Researcher at INESC-PORTO in 1999. He was a Postdoctoral Researcher in Medical Imaging at IEETA-Universidade de Aveiro, Portugal, until September 2006. He has 12 years of experience in computer vision, eight of which in biomedical image and signal processing research. He leads a small research team of around 15 members and either leads or participates in various multidisciplinary projects involving areas such as gastroenterology, cardiology, psychology, biomechanics, and biology. He is currently an Assistant Professor at the Department of Computer Science, Faculty of Sciences, University of Porto. His current research interests include biomedical signal processing and interactive systems for healthcare. He is a Founding Member of the Porto Laboratory of the Instituto de Telecomunicaes, in which he created and currently leads the Interactive Media Group.

Dr. Coimbra is a Technical Advisor of the Portugal Chapter of the IEEE Engineering and Medicine Society, a EURASIP Local Liason Officer and member of the Scientific Committee of the Master in Medical Informatics of the University of Porto.